Reactions of $Cu^+(^1S, ^3D)$ with CH_3Cl, CH_2ClF, $CHClF_2$, and $CClF_3$

William S. Taylor,* Cullen C. Matthews, and Kristin S. Parkhill

Department of Chemistry, University of Central Arkansas, Conway, Arkansas 72035

Received: August 28, 2004; In Final Form: October 17, 2004

The reactions of gas-phase $Cu^+(^1S)$ and $Cu^+(^3D)$ with CH_3Cl, CH_2ClF, $CHClF_2$, and $CClF_3$ are examined using the drift cell technique at 3.5 Torr. State-specific product channels and overall bimolecular rate constants for depletion of the two Cu^+ states are determined using electronic state chromatography. $Cu^+(^1S)$ participates exclusively in association with all four neutrals, whereas Cl abstraction is the dominant product channel for $Cu^+(^3D)$. The resulting $CuCl^+$ product subsequently abstracts Cl^- in a secondary process. Tertiary reactions are also observed, which include both hydride abstraction (with CH_3Cl) and fluoride abstraction (with the fluorinated neutrals). All product channels can be understood in terms of the known thermochemical and quantum mechanical (i.e., spin) requirements. $Cu^+(^1S)$ is depleted by all four neutrals at 30% to 40% of the ADO rate under these conditions, whereas $Cu^+(^3D)$ is observed to react at approximately 80% of the ADO rate with CH_3Cl, CH_2ClF, and $CHClF_2$. Reaction of excited state Cu^+ with $CClF_3$ occurs at only 7% of the ADO rate. The behavior of $Cu^+(^3D)$ is consistent with a mechanism in which formation of $CuCl^+$ occurs exclusively on the triplet surface via a mechanism in which the metal ion must interact exclusively with Cl.

Introduction

An intriguing characteristic of metal ions is their ability to activate σ-bonds, resulting in species that either occur as or serve as models for intermediates in catalytic mechanisms. In such mechanisms, typically unreactive molecules such as methane are functionalized to yield useful products.[1,2] Such catalytic intermediates are coordinatively unsaturated with respect to the metal and are therefore extremely reactive.[3,4] As a result, detailed information regarding the behavior of these open-shell species is often difficult to obtain in condensed phases. Furthermore, the presence of solvent molecules and other ligating species within the coordination sphere of the metal can alter its reactivity.[4,5] Gas-phase studies of the reactions of transition metal ions with organic compounds can yield insights into intrinsic reactivity while avoiding these complicating effects.

A battery of techniques has been brought to bear in the examination of gas phase metal ion chemistry, resulting in a wealth of thermochemical and dynamic information. These studies have thoroughly illustrated that the outcomes of these reactions can be dramatically influenced by the electronic state of the metal—often to the extent that certain states become unreactive regardless of favorable energetics for a given product channel.[1,3−9] One goal of gas phase transition metal ion studies is that this electronic sensitivity might be exploited to selectively control formation of desired products.[7,9] Research into this electronic dependence has revealed that, provided the energetic requirements for reaction are satisfied, state-specificity can be understood in terms of both orbital occupancy requirements for bonding and conservation of electron spin.[1,6−11]

We have been interested in bimolecular processes occurring in reactions of $Cu^+(^1S)$ and $Cu^+(^3D)$ with a variety of small organic molecules. Numerous studies of the behavior of $Cu^+(^1S)$ have been reported with a variety of neutral species.[12−16] In addition, state-specific comparisons have highlighted differences in the chemistry of $Cu^+(^1S)$ and $Cu^+(^3D)$.[17,18] Activation of the C−H bond in CH_4 represents the prototypical example of C−H bond activation; however, reaction of $Cu^+(^1S)$ with CH_4 resulting in rupture of the C−H bond does not occur under thermalized conditions due to unfavorable energetics. Proton abstraction via $Cu^+(^3D)$ is likewise endothermic, and C−H activation to yield $CuCH_2^+$ is spin-forbidden from $Cu^+(^3D)$. Because of these constraints, we have focused our attention on methane analogues in which molecular rearrangements induced by either $Cu^+(^1S)$ or $Cu^+(^3D)$ are energetically and quantum mechanically possible.

Previous work by others has demonstrated that Cu^+ participates in a number of exothermic processes with polar molecules, including CH_3Cl; however, the electronic state distribution was not always specified.[19−24] We have previously described the results of the reactions of $Cu^+(^1S,^3D)$ with CH_3Br in which the observed bimolecular chemistry can be understood within the context of known reaction energetics and quantum mechanical requirements.[25] In the work described here, we expand our examination of the state-specific reactions of Cu^+ to include CH_3Cl, CH_2ClF, $CHClF_2$, and $CClF_3$. These chlorofluorocarbons (CFCs) and hydrochlorofluorocarbons (HCFCs) are used in such applications as refrigeration and plasma processing. Together, these halocarbons present a variety of substrates for the examination of the potential activation of C−H, C−Cl, and C−F bonds. Further HCFCs and CFCs are regarded as relatively unreactive. Hence, selective activation of bonds in these molecules would be noteworthy.

Cu^+ is well-suited for this study for several reasons. It has a limited number of low-lying excited states compared with earlier transition metal ions; therefore, in the absence of the ability to selectively populate a given state this reduces the number of states sampled for subsequent reaction and simplifies the reaction analysis. Further, the ^1S and ^3D states possess different electronic configurations ($3d^{10}$ and $3d^94s^1$). This allows them to be distinguished on the basis of differences in their mobilities in He using electronic state chromatography.[26]

10.1021/jp046106o CCC: $30.25
Published on Web 12/18/2004

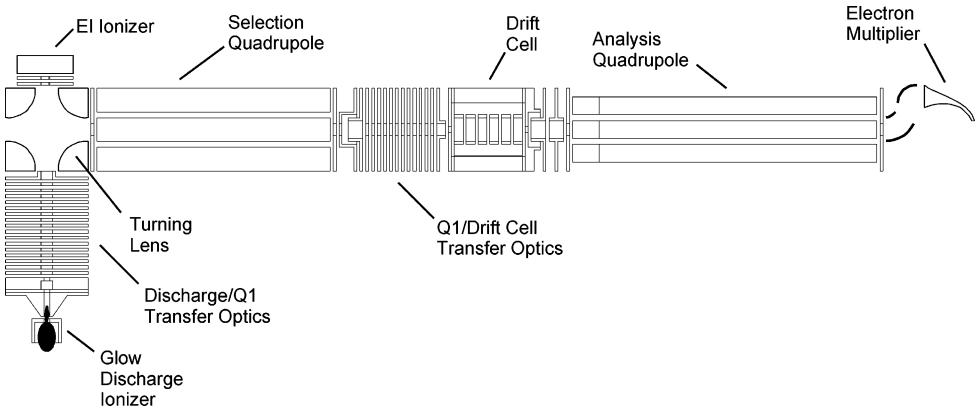

Figure 1. Selected ion drift cell apparatus.

Experimental Section

Instrumental Description. Experiments were carried out using the selected ion drift cell apparatus shown in Figure 1. Cu^+ ions used in this work were produced using a dc glow discharge ion source, which will be discussed in more detail later. The instrument also incorporates an electron impact ion source that was used to produce several of the molecular ions examined here. Ions from either source are directed through a quadrupole deflector (turning lens) and then to a quadrupole mass filter for mass selection. All of the aforementioned components were purchased from Extrel. In this work, the selection quadrupole was operated in two modes. For reactions in which Cu^+ was the reactant ion, Q1 was used as a high-pass filter by operating it in rf-only mode and setting the cutoff mass sufficiently high as to reject unwanted ions produced by the discharge (which consist mainly of lower mass ions produced from residual atmospheric species). This mode of operation produced a reactant ion beam composed exclusively of Cu^+. In examinations of several of the follow-on reactions initiated by Cu^+, Q1 was operated in the normal mass-resolving mode and the required reactant ion in each case (CH_3^+, CH_2F^+, etc.) was generated by electron impact on a suitable precursor species and mass-selected. In either mode, the reactant ion beam is focused onto the entrance aperture of a 4.0 cm drift cell that has been described in detail elsewhere.[27] In typical operation, the drift cell is charged with 3−5 Torr of He and a small partial pressure of the desired reactant neutral. For this work, the mole fraction of the reactant gas in He was on the order of 10^{-4} at a total pressure of 3.5 Torr. Under the conditions employed here, this concentration is sufficiently greater than the ion number density that pseudo-first-order conditions exist with respect to depletion of the reactant ion. Reactant ions are drawn through the drift cell by means of a small electric field maintained by a set of seven guard rings during which time reaction can occur. E/N values for the experiments described here were on the order of 7 Td (1 Td = 1×10^{-17} $cm^2 \cdot V$), and residence times for reactant ions were on the order of 100 μs. These reaction conditions are such that little translational heating occurs and only exothermic or thermoneutral reactions are observed. Temperature control of the drift cell is accomplished via a copper jacket through which heated or cooled gases can be circulated. All of the reactions described in this work were carried out at room temperature. Temperatures within the drift cell are monitored using a Pt−RTD (resistance temperature device). Ions exiting the drift cell are mass-analyzed with the use of a modified Nermag R10-10 quadrupole mass spectrometer. Ions are detected using a Detector Technology model 437 electron multiplier operated in pulse-counting mode. Control of the entire experiment was maintained with the use of the Extrel Merlin Automation Datasystem, which was also utilized to acquire the ion signal in mass spectral format. Arrival time data for electronic state chromatography determinations were collected using an EG&G TurboMCS multichannel scaler set to a channel width of 500 ns. Vacuum conditions suitable for operation of the instrument were maintained using differential pumping in which the chambers containing the selection quadrupole and the drift cell were each pumped independently with 1000 L/s diffusion pumps, whereas the chamber housing the analysis quadrupole was pumped with a 150 L/s diffusion pump.

Metal Ion Source. Cu^+ ions for use in this work were produced by a glow discharge source that has been described previously.[28] Briefly, this ion source produces metal ions via a sputter bombardment process in which ions of a working gas (Ne in this work) are accelerated to a cathode made from the desired metal. Metal atoms are sputtered from the surface of the cathode and diffuse into an intensely luminous region of the discharge known as the negative glow. The metal atoms are then ionized by either Penning ionization via metastables of the working gas, or by electron impact ionization via fast electrons being accelerated from the cathode. Metal ions are sampled directly from the discharge plasma. We have previously demonstrated that this ion source is capable of producing metal ions in excited states as well as in their ground states. Further, excited state populations can be controlled to some extent by manipulation of discharge parameters.[29] In this work, $Cu^+(^3D)$/$Cu^+(^1S)$ ratios were increased or decreased by respectively decreasing or increasing the distance between the sampling aperture and the cathode.

Determination of Cu^+ State Distribution. For the work described here, specific configurations of Cu^+ ions produced in the glow discharge were identified within the drift cell using a technique called electronic state chromatography (ESC), which characterizes them on the basis of the their mobilities in He.[26] ESC is most effective in distinguishing between electronic configurations differing significantly in size, such as those that differ by either the presence or absence of an s electron. The larger size of the s orbital results in a greater repulsive interaction between the ion and the He bath gas, which reduces the number of capture collisions. In terms of the first-row ions, this means that ions with $3d^{n-1}4s^1$ configurations have higher mobilities in the bath gas than those with $3d^n$ configurations. As a consequence, a pulse containing a given metal ion in both configurations will be separated within the drift cell such that the higher mobility configuration arrives at the detector first. Thus, configurations of sufficiently different mobilities appear

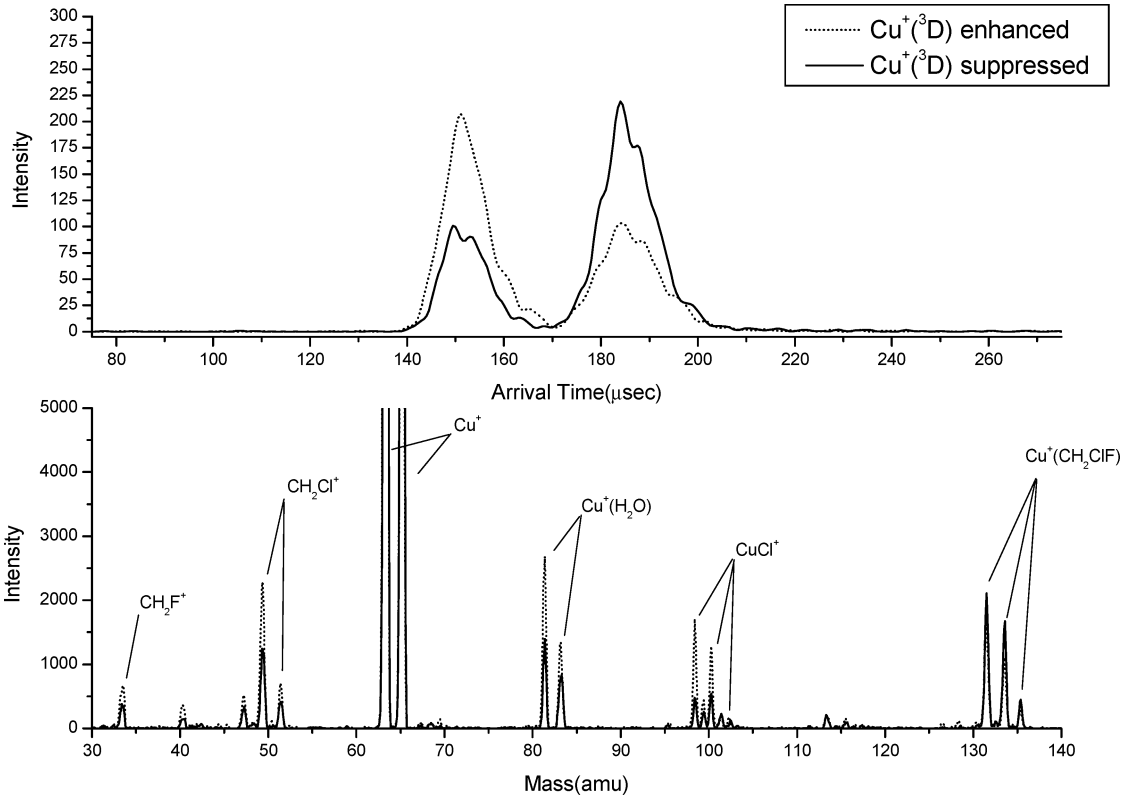

Figure 2. Cu^+ ATDs and comparison spectra for the reaction of $Cu^+(^1S, ^3D)$ with CH_2ClF in which the ion source has been adjusted to either enhance (dotted line) or suppress (solid line) production of $Cu^+(^3D)$. $T = 300$ K; $E/N = 7.3$ Td; $X_{CH_2ClF} = 7.6 \times 10^{-5}$.

as different peaks in an arrival time distribution (ATD). Ion mobilities used in assigning configurations were obtained from the ATDs by measuring the flight time of the different configurations as a function of the reciprocal of the drift voltage as has been described.[26]

ESC analysis of Cu^+ extracted from the discharge indicates the presence of two configurations. Mobility measurements indicate that these correspond to $3d^{10}$ and $3d^94s^1$. A previous analysis of excited states formed in the glow discharge suggests that this ion source is capable of producing excited metal ion states with energies up to approximately 11.8 eV above the atom ground state.[29] For Cu^+, this energy range includes the $^1S(3d^{10})$ ground state, as well as the $^3D(3d^94s^1)$ and $^1D(3d^94s^1)$ excited states, which lie 2.842 eV (averaged over *J*-levels) and 3.257 eV above the ^1S state. Cu^+ states above ^1D are not metastable and would not have sufficient lifetimes to influence the reactions reported here. The low-mobility feature in our Cu^+ ATDs is undoubtedly the ^1S ground state, but because the first and second excited states are indistinguishable on the basis of their mobilities, we cannot rule out the presence of both within the high mobility feature on the basis of ESC alone. Our previous examination of ionization/excitation within the discharge has suggested that excited atomic ions extracted from the discharge are produced primarily by an electron impact process and, in the absence of any preferential depletion mechanism(s), the relative populations of the excited metal ions will be dependent on the electron energy distribution function at the point of sampling within the discharge.[29] Thus, though some amount of $Cu^+(^1D)$ may be present in the $3d^94s^1$ (high mobility) feature, it is likely that the major contributors to this configuration are the energetically more accessible $^3D_{3,2,1}$ states. We have tested for the presence of $Cu^+(^1D)$ with the use of bracketing charge-transfer reactions with C_3H_8 (IP = 10.94 eV) and C_3F_6 (IP = 10.60 eV). The ionization potential of C_3H_8 falls between the sum of the IP for Cu and the additional energy for the $^3D_1$ and $^1D_2$ states (10.70 and 10.98 eV, respectively). Thus, though $Cu^+(^1D)$ is energetically capable of charge transferring with this neutral, the $Cu^+(^3D)$ spin−orbit states are not. Similarly, only the $^1D_2$ and $^3D_1$ Cu^+ states are energetically capable of inducing charge-transfer with C_3F_6. Product spectra in these reactions indicated no significant amount of charge-transfer products, suggesting that the $3d^94s^1$ Cu^+ configuration that we observe contains little or no contribution from states above $^3D_2$.

Copper cathodes used as sputter targets were fashioned from used oxygen-free copper gaskets into 5.0 mm diameter rods. Neon used as the discharge gas was obtained from Matheson Tri-Gas Inc. with a purity of 99.999%. Helium used as the buffer gas in the drift cell was obtained from Air Products Inc. with a purity of 99.9999%. CH_3Cl and $CHClF_2$ were purchased from Matheson Tri-Gas Inc. with purities of 99.9% and 99.8%, respectively. CH_2ClF and $CClF_3$ were both 99% pure and were obtained from Synquest Gases Inc.

Results and Discussion

State-specificity with respect to product formation was determined using two methods: (1) acquiring product mass spectra while manipulating reactant ion state distributions and (2) correlating reactant and product ATDs. In the first method, the discharge conditions were first adjusted such that production of $Cu^+(^3D)$ was minimized. A continuous beam of the reactant ion was then injected into the drift cell containing halocarbon/He mixtures described above. Mass spectra accumulated under these conditions were then compared to those obtained when the discharge was adjusted to produce more of the ^3D state. This is illustrated for the reaction of Cu^+ with CH_2ClF in Figure 2 where the two spectra are overlaid. These spectra clearly show that production of several species is enhanced when ionization conditions are manipulated to increase production of $Cu^+(^3D)$.

TABLE 1: Ionic Products Arising from Cu^+ Precursor States and State-Specific Overall Rate Constants for Cu^+ Depletion

	$Cu^+(^1S)$			$Cu^+(^3D)$		
reactant neutral	ionic product	k_{obs} ($x10^{-10}$)[a]	k_{obs}/k_{ADO}[b]	ionic product	k_{obs} ($x10^{-9}$)[a]	k_{obs}/k_{ADO}[b]
CH_3Cl	$Cu^+ \cdot CH_3Cl$	7.1 ± 0.7	0.40	$CuCl^+$ CH_3^+ CH_2Cl^+ $Cu^+ \cdot CH_3Cl$	1.4 ± 0.2	0.79
CH_2ClF	$Cu^+ \cdot CH_2ClF$	4.9 ± 1.1	0.29	$CuCl^+$ CH_2F^+ CH_2Cl^+ $Cu^+ \cdot CH_2ClF$	1.4 ± 0.2	0.82
$CHClF_2$	$Cu^+ \cdot CHClF_2$	4.5 ± 0.4	0.31	$CuCl^+$ CHF_2^+ $CHClF^+$ $Cu^+ \cdot CHClF_2$	1.1 ± 0.1	0.77
$CClF_3$	$Cu^+ \cdot CClF_3$	3.1 ± 0.1	0.31	$CuCl^+$ CF_3^+ CF_2Cl^+ $Cu^+ \cdot CClF_3$	$.066 \pm 0.016$	0.07

[a] Units of $cm^3 \cdot molecule^{-1} \cdot s^{-1}$. [b] Fraction of collision rate predicted by average dipole orientation model; see ref 39.

Products formed in greater abundance under these conditions include $CuCl^+$, CH_2Cl^+, and CH_2F^+. Additionally, peaks corresponding to $Cu^+ \cdot CH_2ClF$ are somewhat enhanced when $Cu^+(^3D)$ is suppressed; however, as we will show, subsequent tests reveal that this product mass is contributed to by both Cu^+ states. Species arising from each Cu^+ state are summarized in Table 1.

These initial analyses indicate that $Cu^+(^1S)$ participates exclusively in association under these conditions with these neutrals and that all of the observed bimolecular chemistry arises from $Cu^+(^3D)$ via some means. No evidence of dehydrohalogenation resulting in the formation of an ionic copper carbene species was observed. With respect to CH_3Cl, formation of $CuCH_2^+$ is not possible from the ground state on the basis of thermochemistry and is spin-forbidden from the ^3D state despite favorable energetics.[4] Similar spin restrictions will occur via $Cu^+(^3D)$ for carbene formation for all of these neutrals. Binding energies for the halogenated copper carbene species are not known; therefore energetic arguments to explain the lack of formation of these species via $Cu^+(^1S)$, though plausible, become speculative. Interestingly, Cu^+-CH_3 was not observed to proceed from $Cu^+(^3D)$ in the Cu^+/CH_3Cl system even though no energetic or quantum mechanical prohibitions exist.[4] Likewise, none of the fluorinated analogues of the Cu^+-methyl moiety were formed with the other neutrals. We have previously reported the same behavior in the reaction of $Cu^+(^3D)$ with CH_3Br and concluded that this product channel is prevented on the basis of unfavorable kinetics.[25] The results of this work suggest that similar kinetic barrier to the formation of the methylated copper ion exist in the systems discussed here.

Although useful in providing an overall picture of state-specific product formation, comparison spectra do not explicitly indicate that $Cu^+(^3D)$ is the *direct* precursor for the bimolecular products listed in Table 1—only that $Cu^+(^3D)$ is ultimately responsible for their formation. Thermochemical changes for reactions that would originate from each Cu^+ state can be calculated (depending on the specific reaction) from available bond strengths and ionization potentials according to the following equation:

$$\Delta E = D_{0(RN)} - D_{0(Cu-X)} - IP_{(Cu)} + IP_{(PI)} - E_{state} \quad (1)$$

where $D_{0(RN)}$ and $D_{0(Cu-X)}$ represent the bond dissociation energies for the bond broken in the reactant neutral and the bond formed between Cu and either Cl, F, or H, respectively. E_{state} is the energy of the Cu^+ state relative to the ion ground state. Thermochemical calculations for reactions of excited state Cu^+ reactions utilize $E_{state} = 2.833$ eV (the energy of the $^3D_2$ spin−orbit state) because our charge-transfer bracketing results indicate that states with energies above this are not present in the drift cell. $IP_{(PI)}$ designates the ionization potential for neutral precursor to the product ion. Several values have been reported for the ionization potentials of many of the halocarbon radicals related to the reactions described here. In two cases (CHF_2 and $CClF_2$) our results suggest that a particular value or range of values be used (discussed below). These two radicals will result from C−Cl bond cleavage in $CHClF_2$ and CCl_2F_2, both of which have had wide use as refrigerants and foaming agents. Thus, additional information regarding the ionization energetics of their photolytic radical products may play an important role in understanding their ultimate environmental fates. The ionization potentials used to calculate thermochemical changes in this work are given in Table 2.[30−34]

TABLE 2: Ionization Potentials Used in Thermochemical Calculations

species	IP (eV)	ref
Cu	7.72638	30
CuCl	10.7	31
CH_3	9.84	30
CH_2Cl	8.75, 8.80	31, 32
CHClF	8.37, 8.81, 9.16	32, 33
CH_2F	8.90, 9.04, 9.16, 9.35	31, 32, 34
CHF_2	8.74, 8.78, 9.45, 10.5	31, 33
$CClF_2$	9.0	33
CF_3	8.5, 8.60, 8.76, 8.9, 9.11, 9.14, 9.17, 9.25, 9.3, 9.5, 9.8	31−34

Using these values, the thermochemistry required for direct formation of each of the observed product ions listed in Table 1 from each Cu^+ state is summarized in Table 3, along with possible spin changes. Ranges in these calculated values reflect ranges in the ionization potentials listed in Table 2. Primary product channels that can be excluded on the basis of either energetics or spin have been identified accordingly and therefore cannot be the means by which those particular product ions are formed. It is clear that unfavorable energetics is the reason that none of the observed bimolecular products arise from the ground state. Conversely, although the product channels observed to arise from $Cu^+(^3D)$ are all energetically favorable, quantum mechanical requirements for conservation of electron spin argue against direct formation of all bimolecular products except $CuCl^+$ from this state. This strongly suggests that all other product ions result from subsequent reaction steps.

TABLE 3: Primary Product Channel Requirements

	reactant ion	product channel	thermochemistry (kJ/mol)[a]	$\Delta\Sigma$[a]	primary?
CH_3Cl	(^{1}S) Cu^+	$CuCl^+ + CH_3$	256	0,±1	N
		$CH_3^+ + CuCl$	173	0	N
		$CH_2Cl^+ + CuH$	243 to 247	0	N
	(^{3}D) Cu^+	$CuCl^+ + CH_3$	−17	±2,±1,0	Y
		$CH_3^+ + CuCl$	−100	±1	N
		$CH_2Cl^+ + CuH$	−30 to −25	±1	N
CH_2ClF	(^{1}S) Cu^+	$CuCl^+ + CH_2F$	256	0,±1	N
		$CH_2Cl^+ + CuF$	148 to 153	0	N
		$CH_2F^+ + CuCl$	82 to 125	0	N
	(^{3}D) Cu^+	$CuCl^+ + CH_2F$	−17	±2,±1,0	Y
		$CH_2Cl^+ + CuF$	−124 to −120	±1	N
		$CH_2F^+ + CuCl$	−191 to −148	±1	N
$CHClF_2$	(^{1}S) Cu^+	$CuCl^+ + CHF_2$	269	0,±1	N
		$CHClF^+ + CuF$	114 to 190	0	N
		$CHF_2^+ + CuCl$	80 to 250	0	N
	(^{3}D) Cu^+	$CuCl^+ + CHF_2$	−4	±2,±1,0	Y
		$CHClF^+ + CuF$	−159 to −83	±1	N
		$CHF_2^+ + CuCl$	−193 to −23	±1	N
$CClF_3$	(^{1}S) Cu^+	$CuCl^+ + CF_3$	264	0,±1	N
		$CF_3^+ + CuCl$	52 to 177	0	N
		$CF_2Cl^+ + CuF$	199	0	N
	(^{3}D) Cu^+	$CuCl^+ + CF_3$	−9	±2,±1,0	Y
		$CF_3^+ + CuCl$	−221 to −95	±1	N
		$CF_2Cl^+ + CuF$	−73	±1	N

[a] Assumes products formed in their ground states.

TABLE 4: Observed Secondary and Tertiary Reactions and Related Thermochemistry

	reactant ion	product channel	reaction sequence[a]	thermochemistry (kJ/mol)
CH_3Cl	$CuCl^+$	$CH_3^+ + CuCl_2$	secondary chloride abstraction	−25[b]
		$CH_2Cl^+ + CuHCl$	possible secondary hydride abstraction	*c*
	CH_3^+	$CH_2Cl^+ + CH_4$	tertiary hydride abstraction	−122 to −118
CH_2ClF	$CuCl^+$	$CH_2F^+ + CuCl_2$	secondary chloride abstraction	−116 to −73[b]
		$CH_2Cl^+ + CuClF$	possible secondary fluoride abstraction	*c*
	CH_2F^+	$CH_2Cl^+ + CH_2F_2$	tertiary fluoride abstraction	−94 to −46
$CHClF_2$	$CuCl^+$	$CHF_2^+ + CuCl_2$	secondary chloride abstraction	−118 to 52[b]
		$CHClF^+ + CuClF$	possible secondary fluoride abstraction	*c*
	CHF_2^+	$CHClF^+ + CHF_3$	tertiary fluoride abstraction	−233 to −29
$CClF_3$	$CuCl^+$	$CF_3^+ + CuCl_2$	secondary chloride abstraction	−146 to −20[b]
		$CF_2Cl^+ + CuClF$	possible secondary fluoride abstraction	*c*
	CF_3^+	$CClF_2^+ + CF_4$	tertiary fluoride abstraction	−126 to −1

[a] Reaction steps refer to Figure 3. [b] ClCu−Cl bond strength from ref 36. [c] Thermochemistry not known. Specific thermochemical requirements for possible secondary reactions discussed in text.

A better assessment of the role of both Cu^+ states in the formation of each of the products can be obtained by correlating product ATDs to those of the two Cu^+ states using a variation of the ESC experiment outlined previously.[35] The Cu^+ ATD is first collected under the same drift cell conditions as the reaction of interest minus the reactant neutral. A small amount of the reactant neutral is then admitted into the drift cell and the mass filter is tuned to the desired product ion mass while the reactant ion beam is pulsed. The ATDs for both species are then corrected to account for differences in flight times through the quadrupole, and then overlaid. The reactant ion can be converted into the product at any point within the drift cell, but a product ion formed near the exit of the drift cell will exhibit a flight time characteristic of the reactant ion producing it. Thus, the shortest drift time of a product ion with a mobility lower than that of the reactant (as was the case for primary product channels observed here) will correspond to the shortest drift time of the reactant ion producing it. In this way, possible reactant ion precursors for most of the products observed in this work were identified and are summarized in Table 4 along with thermochemical changes for each product channel according to

$$\Delta E = D_{0(RN)} - D_{0(PN)} + IP_{(PI)} - IP_{(RI)} \qquad (2)$$

This is a more general form of the equation used to calculate the energetic requirements listed in Table 3 in which we have made the assumption that none of the reactant ions is in an excited state; therefore the E_{state} term in eq 1 is not included. As in eq 1, $D_{0(RN)}$ and $D_{0(PN)}$ are the dissociation energies of the bonds either broken or formed in the reactant neutral and product neutral respectively, and $IP_{(PI)}$ and $IP_{(RI)}$ are the ionization potentials of the neutral precursors of the product and reactant ions.[30−36] As in Table 3, ranges in reaction thermochemistry reported in Table 4 occur as a result of more than one value reported for $IP_{(PI)}$ and $IP_{(RI)}$. Details regarding specific reactions are discussed below; however, in all cases, product ATDs are consistent with the idea that most of the product species in Table 1 must arise in follow-on steps initiated by $CuCl^+$ and suggest the general reaction scheme given in Figure 3 for depletion of $Cu^+(^3D)$ in which reactions observed in at least one of the systems discussed here are included. In this process, $Cu^+(^3D)$ initially abstracts a chlorine atom from the halocarbon resulting in the spin-allowed formation of $CuCl^+$. Formation of a species with a mass corresponding to that of the adduct was also observed with all four neutrals as a minor product channel originating from $Cu^+(^3D)$; however, as discussed below, we feel that this species is a secondary product

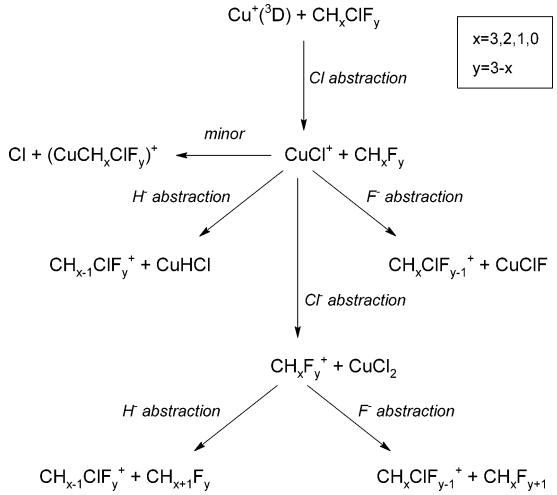

Figure 3. Generalized reaction scheme illustrating product channels observed to be initiated by $Cu^+(^3D)$ with the halocarbons in this work. Not all products are observed with every neutral.

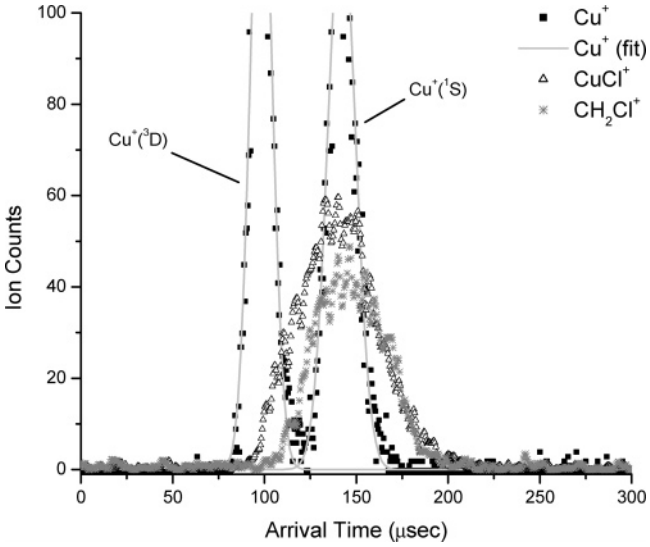

Figure 4. Cu^+, $CuCl^+$, and CH_2Cl^+ ATDs for the reaction of $Cu^+(^1S, ^3D)$ with CH_3Cl. Cu^+ ATDs fit to Gaussians. $T = 300$ K; $E/N = 7.3$ Td; $X_{CH_3Cl} = 9.6 \times 10^{-5}$.

of reaction with $CuCl^+$ rather than a direct association product arising from $Cu^+(^3D)$. Depending on the specific halocarbon, $CuCl^+$ can potentially participate in up to three parallel spin-allowed halide abstractions resulting in the formation of three different carbocation species. In the reactions examined here, the secondary chloride abstraction product ($CH_xF_y^+$) was subsequently observed to abstract either H^- (with CH_3Cl) or F^- (with the fluorinated neutrals) in a tertiary reaction step.

CH_3Cl. As indicated in Table 1, association is the only process exhibited by $Cu^+(^1S)$ with this neutral, whereas three bimolecular products occur in the presence of $Cu^+(^3D)$. Product ATDs for $CuCl^+$ and CH_2Cl^+ are given in Figure 4, which clearly originate prior to the Cu^+ ATD feature arising from the singlet state. Although also observed as a product originating from $Cu^+(^3D)$, CH_3^+ intensities were inadequate for ATD acquisition. Although formation of all three bimolecular products is spin-allowed via $Cu^+(^1S)$, all are endothermic and therefore not accessible under these reaction conditions. Conversely, the thermochemistry for production of $CuCl^+$, CH_3^+, and CH_2Cl^+ via $Cu^+(^3D)$ is favorable for all three, but only in the case of $CuCl^+$ is spin conserved from $Cu^+(^3D)$, thus preventing direct Cl^- and H^- abstraction by this Cu^+ state. CH_3^+ and CH_2Cl^+

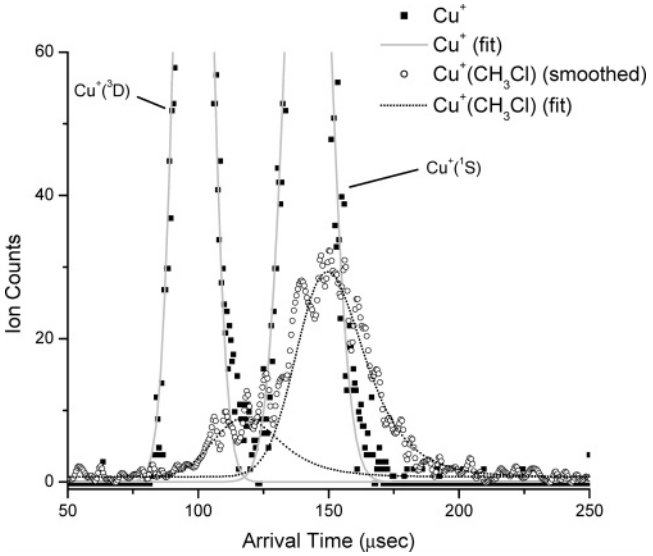

Figure 5. Cu^+ and $Cu^+ \cdot CH_3Cl$ ATDs for the reaction of $Cu^+(^1S, ^3D)$ with CH_3Cl. Reactant and product ATDs have both been fit to two Gaussians. $T = 300$ K; $E/N = 7.3$ Td; $X_{CH_3Cl} = 9.6 \times 10^{-5}$.

must therefore be formed in subsequent reaction steps for which energetic requirements are satisfied. In the case of CH_3^+, the available thermochemistry (Table 4) suggests that this ion is likely formed in a secondary process in which $CuCl^+$ is the precursor. In addition, the CH_2Cl^+ ATD in Figure 4 originates later than both the $Cu^+(^3D)$ ATD and the $CuCl^+$ ATD, suggesting that it is produced in a follow-on step either as a secondary product from $CuCl^+$ or as a tertiary product from CH_3^+. Production of CH_3^+ from CH_2Cl^+ is precluded on the basis of energetics. We have confirmed that formation of CH_2Cl^+ from CH_3^+ does occur in an independent experiment in which methyl cation was produced by electron impact ionization of CH_3Br, mass-selected by Q1 and subsequently injected into the drift cell. Mass spectra were then collected in the presence of CH_3Cl which conclusively show that CH_2Cl^+ is a product of CH_3^+. This spectrum also shows that $CH_3^+ \cdot CH_3Cl$ is also formed in a parallel process. This cluster is also observed in small amounts when $Cu^+(^3D)$ is the reactant ion, thus providing further indication that CH_3^+ is being formed from excited Cu^+ via some means. The low abundance of CH_3^+ in the Cu^+/CH_3Cl system suggests that this ion is efficiently converted to CH_2Cl^+ and $CH_3^+ \cdot CH_3Cl$. CH_2Cl^+ intensities continue to grow in at progressively higher extents of reaction, indicating that this ion is a terminal product; however, our results cannot conclusively rule out the additional formation of CH_2Cl^+ as a secondary product from $CuCl^+$ via hydride abstraction. The available thermochemistry indicates that the strength of the (CuCl)−H bond formed in this process must be >233 kJ/mol for it to occur in the near-thermal reaction environment of the drift cell. If this species is one in which the hydrogen is bonded to the copper atom, the magnitude of this binding energy is comparable to that of diatomic Cu−H (277.8 kJ/mol). We therefore feel that parallel production of CH_2Cl^+ in this manner cannot be excluded as a possible reaction channel. Association of $Cu^+(^1S)$ with CH_3Cl to yield the adduct species must proceed via a three-body process in which the initial ion/neutral pair is stabilized by collision with He. Participation of $Cu^+(^1S)$ in the formation of this product is consistent with our previous work with CH_3Br in which association occurred almost exclusively via the ground state with minor contributions from $Cu^+(^3D)$ seen only at low temperature.[25] In this case however, the product ATD (Figure 5) for the adduct indicates that $Cu^+(^3D)$ also

contributes to a product at this mass at room temperature. This observation is consistent with a previously−reported result for this reaction carried out in an ICR cell.[19] In that study, a species with the mass of $Cu^+ \cdot CH_3Cl$ was shown to arise as a secondary product in an inefficient bimolecular process in which $CuCl^+$ abstracts CH_3 from CH_3Cl. Because we have shown that $CuCl^+$ arises exclusively from $Cu^+(^3D)$, some fraction of the Cu^+ in this earlier study must have been in this state. We have also shown that three-body association in the Cu^+/CH_3Br system is observed via $Cu^+(^3D)$ only at low temperatures, indicating a weaker interaction with $Cu^+(^3D)$.[25] Given a similar weak electrostatic interaction between $Cu^+(^3D)$ and these neutrals, association at room temperature would not be competitive at this pressure with the relatively efficient bimolecular formation of $CuCl^+$ as evidenced by the observed rate of depletion of $Cu^+(^3D)$. Thus, we feel that it is likely that the portion of the $Cu^+ \cdot CH_3Cl$ ATD in Figure 5 correlating to $Cu^+(^3D)$ is produced via the same bimolecular pathway as that reported in the previous ICR study, rather than via a three-body process originating directly from $Cu^+(^3D)$.

CH_2ClF. Analysis of product ATDs in this reaction are again consistent with the overall state-specificity summarized in Table 1. Reaction of $Cu^+(^1S)$ with this neutral yields an association product exclusively, whereas $Cu^+(^3D)$ initiates bimolecular channels resulting in the rupture of both C−Cl and C−F bonds. Reactions induced by $Cu^+(^3D)$ with this neutral appear to be analogous to those observed with CH_3Cl. The combined requirements of exothermicity and conservation of spin (Table 3) again suggest that $CuCl^+$ is the only species to be produced directly from $Cu^+(^3D)$ whereas CH_2F^+ and CH_2Cl^+ are produced in later steps (Table 4). $CHClF^+$ resulting from hydride abstraction is not observed in any significant amount. Because CH_2Cl^+ is thermochemically prohibited from producing CH_2F^+ under thermalized conditions, CH_2F^+ must arise as a secondary product of via Cl abstraction by $CuCl^+$. Tertiary formation of CH_2Cl^+ was independently verified by carrying out electron impact fragmentation on CH_3F to form CH_2F^+, which was subsequently injected into the drift cell containing the reactant mixture. Here also, the parallel formation of CH_2Cl^+ directly from $CuCl^+$ cannot be excluded. This fluoride abstraction path becomes thermochemically accessible only if the F−CuCl binding energy is at least 275 kJ/mol in the neutral species. Given that the bond strength in diatomic CuF is approximately 8% stronger than that for diatomic CuCl (413.4 kJ/mol vs 382.8 kJ/mol), it seems reasonable to expect that the F−CuCl bond strength will exceed the reported 293.7 kJ/mol bond strength in Cl−CuCl.[36] For this reason, it seems possible that CH_2Cl^+ can be produced in this reaction as both a secondary and a tertiary product. As in the case of CH_3Cl, product ATDs indicate minor contributions to a product with the mass of the adduct from $Cu^+(^3D)$ consistent with formation of a bimolecular secondary product via $CuCl^+$.

$CHClF_2$. Following the initial formation of $CuCl^+$ from $Cu^+(^3D)$, subsequent products are observed that result from both chloride and fluoride abstractions from $CHClF_2$. Product ATDs indicate that $CuCl^+$ and CHF_2^+ both correlate to $Cu^+(^3D)$ and that $CHClF^+$ occurs in a later step. Because direct formation of CHF_2^+ from $Cu^+(^3D)$ is spin-forbidden, we conclude that this species is formed in a secondary reaction via Cl^- abstraction by $CuCl^+$. Observation of this product in this reaction step indicates that the ionization energy for CHF_2 radical must be less than 961 kJ/mol. As listed in Table 2, this ionization potential has been reported to be as high as 1013 kJ/mol (10.5 eV).[33] Our observation of CHF_2^+ suggests that this value is too high because it predicts that formation of this ion would be endothermic by 52 kJ/mol (see Table 4) and therefore not observed in our apparatus.

Formation of $CHClF^+$ by fluoride transfer to CHF_2^+ is thermochemically possible for all reported values for the ionization potential for CHF_2. As was done in the previous two reactions, this follow-on reaction was verified in a separate experiment in which CHF_2^+ was produced in the EI source of the instrument from $CHClF_2$, then injected into the drift cell to react with $CHClF_2$. Mass spectra of this reaction clearly indicate that $CHClF^+$ is formed directly from CHF_2^+. We thus conclude that $CHClF^+$ is formed in a tertiary reaction step in the process initiated by $Cu^+(^3D)$. As in the previous two neutrals, $Cu^+(^3D)$ contributes to a small portion of the signal observed at the mass of the association product, the structure of which is undetermined. Again, product ATDs for this species are not inconsistent with the idea that the portion of this mass originating from $Cu^+(^3D)$ is actually formed from $CuCl^+$ in a bimolecular process. This reaction sequence also includes the possible formation of $CHClF^+$ via fluoride abstraction by $CuCl^+$. The energetic requirements for the F−CuCl binding energy necessary for this to occur can be calculated as was done with CH_2ClF. A 76 kJ/mol range in the reported values for the ionization potential for CHClF results in possible lower limits on the F−CuCl binding energy of 241−317 kJ/mol. This uncertainty makes it difficult to draw conclusions regarding the existence of this product channel; however, these binding energies are similar in magnitude to that required in the CH_2ClF system so we likewise include it as a possibility.

Notably, $CClF_2^+$ is not observed. Because formation of this ion is spin-allowed from $CuCl^+$, CHF_2^+, and $CHClF^+$, unfavorable energetics are the likely inhibiting factors. As has been noted above, the energetics for hydride abstraction includes the ionization potential for the product ion. In the case of $CClF_2$, two significantly different values (868 and 1254 kJ/mol) have been reported.[33] As described below, we feel that the lower of these two values is more accurate and is used here. Accordingly, the apparent endothermicity of hydride abstraction by $CuCl^+$ allows us to establish an upper limit on the H−CuCl binding energy of 257 kJ/mol.

$CClF_3$. Analysis of product ATDs indicates that this reaction proceeds in a manner analogous to that of CH_3Cl where $Cu^+(^1S)$ associates, whereas $Cu^+(^3D)$ initiates a series of reaction steps beginning with the formation of $CuCl^+$. As in the other reactions, a minor component of the $Cu^+ \cdot CClF_3$ signal is observed to originate ultimately with $Cu^+(^3D)$, consistent with formation of a product species of the same mass as the association product but differing in structure via $CuCl^+$. The relative positions of the remaining product ATDs are consistent with CF_3^+ being formed as a secondary product, which in turn reacts to yield CF_2Cl^+ in a tertiary step. Precise determination of the thermochemical changes that will occur in this fluoride abstraction are not possible because a number of values have been reported for the ionization potential of CF_3; however, this tertiary reaction step provides some insight into discriminating between the two values of 868 and 1254 kJ/mol, which have been put forth for $CClF_2$. The lower value was measured using charge inversion energy loss spectroscopy with a reported error of ±48 kJ/mol.[37] The higher reported value was obtained indirectly from data obtained in charge-stripping experiments in which $CClF_2^+$ was converted to $CClF_2^{2+}$. This value has an error of ±96 kJ/mol (1 eV) and includes several assumptions that limit its accuracy.[38] If the higher value is used to calculate thermochemical changes in our work, formation of $CClF_2^+$ via

fluoride abstraction by CF_3^+ is endothermic for all reported values of the ionization potential of CF_3. Because our results indicate that this reaction does in fact occur, we conclude that the higher ionization potential for $CClF_2$ is too high. Using the lower value, we then calculate that parallel formation of $CClF_2^+$ from $CuCl^+$ can occur if the F−CuCl binding exceeds 326 kJ/mol. Lacking any quantitative rationale to reject this value, and because it is not inconsistent with the lower limits required for the same process with the other fluorinated species examined here, this product channel cannot be excluded on this basis.

Reaction Kinetics. The relative efficiency with which each Cu^+ was consumed by all four neutrals was assessed by collecting reactant ATDs in the presence of varying concentrations of the halocarbons in He. Because the neutral number density within the drift cell exceeds that of the ions by several orders of magnitude, pseudo-first-order conditions exist with respect to depletion of Cu^+. It therefore becomes possible to measure the overall reaction rate constants by monitoring the depletion of $Cu^+(^3D)$ and $Cu^+(^1S)$ via ESC as a function of halocarbon number density at fixed residence time in the drift cell. Residence times for both Cu^+ states were determined by the following equation:

$$t_R = \frac{L^2}{VK} \tag{3}$$

where L is the length of the drift cell (in this case 4.0 cm), V is the drift voltage, and K is the mobility for the specific copper state in question at the conditions of T and P extant within the drift cell. Mobilities for both Cu^+ states can be readily calculated from reduced mobilities that have been previously measured.[26,29] Logarithmic plots of Cu^+ intensity as a function of halocarbon density exhibit linear behavior for both Cu^+ states consistent with first-order kinetics. Overall rate constants are calculated from the slope of these decays and are summarized in Table 1 for each Cu^+ state, along with fractions of the limiting values, as predicted by the ADO (average dipole orientation) model.[39] With the exception of $CClF_3$, these neutrals react 2 to 3 times as fast with $Cu^+(^3D)$ as with $Cu^+(^1S)$ under these conditions. Because $Cu^+(^1S)$ exhibits association exclusively, the observed rate constant is expected to be pressure-dependent, although this was not explored here. The ADO rate in this case represents what the observed rate would be provided the reaction is carried out under pressures at which stabilizing collisions with He occur faster than the initial $Cu^+(^1S)$/halocarbon encounter complex can dissociate back to reactants. The low values for the observed rate constants relative to the ADO rate constants are an indication that the pressure used here is too low for association to proceed with every encounter between $Cu^+(^1S)$ and the neutral. Because product formation in the reactions of $Cu^+(^3D)$ is the result of bimolecular processes, direct comparison to the ADO rate constant provides information regarding barriers to reaction. The observation that $Cu^+(^3D)$ reacts with three of the four halocarbons at a large percentage of the ADO rate indicates efficient access on the triplet surface to the product channel resulting in $CuCl^+$ for these halocarbons. Further, the notable reduction in the rate of depletion of $Cu^+(^3D)$ by $CClF_3$ points to a barrier in the $CuCl^+$ exit channel for this neutral.

Mechanistic Interpretations. The kinetic results reported above, along with the fact that $CuCl^+$ is the only significant primary product observed to be formed from $Cu^+(^3D)$ provide useful information regarding the potential energy surface that governs the behavior of these reactions. With respect to the Cu^+/CH_3Cl system, the absence of Cu^+-CH_3 despite favorable energetics suggests that formation of this species is prevented

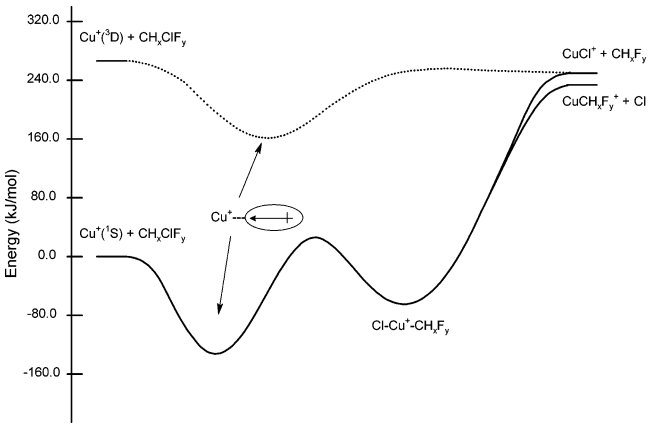

Figure 6. Qualitative potential energy surfaces for the reaction of $Cu^+(^1S, ^3D)$ with CH_3Cl, CH_2ClF, $CHClF_2$, and $CClF_3$. Reaction energetics have been calculated on the basis of bond-additivity for the Cu^+/CH_3Cl system. The singlet surface is given by the solid line and the triplet surface is indicated by a dotted line.

on the basis of kinetics and indicates a mechanism where the metal interacts exclusively with the halide rather than inserting into the CH_3-X bond. Such a direct mechanism has been proposed by Armentrout and co-workers to describe the behavior of specific states of Fe^+, Co^+, and Ni^+ with methyl halides where the ionic metal halide proceeds directly from an ion−dipole complex in which the halide on the neutral is oriented toward the metal.[40,41] We believe that our results are consistent with this idea, and we propose a similar qualitative potential energy surface to describe these Cu^+ reactions (Figure 6), in which the overall energetics associated with product formation has been estimated on the basis of bond-additivity for the case where CH_3Cl is the neutral. In this scenario, reaction on both surfaces results in an initial association complex in which the negative end of the dipole is oriented toward Cu^+. The presence of the 4s electron in $Cu^+(^3D)$ results in a more repulsive interaction and a shallower well for this initial ion−dipole complex than that of the singlet species. Presumably, the association products observed to arise from the singlet state occur via collisional-relaxation of the singlet ion−dipole complex via He. Given that the necessary energetic requirements are satisfied, this association process competes with the formation of an insertion intermediate that can then decompose into either $CuCl^+$ or $CuCH_3^+$. In our case, however, the endothermicity of both of these product channels arising from $Cu^+(^1S)$ prevents either of these processes even though spin is conserved throughout. As a consequence, association is the only product channel observed for $Cu^+(^1S)$. Formation of either $CuCH_3^+$ or $CuCl^+$ is exothermic from $Cu^+(^3D)$, but reaction on the triplet surface precludes the formation of the insertion intermediate. Instead, formation of $CuCl^+$ proceeds directly from the ion−dipole intermediate in a process with little or no activation barrier, as indicated by the rapid rate of depletion of $Cu^+(^3D)$. The fact that reaction of $Cu^+(^3D)$ proceeds with similar efficiency with CH_2ClF and $CHClF_2$ suggests a similar direct process for Cl abstraction with the HCFCs. We therefore conclude that even though the dipole in CH_2ClF and $CHClF_2$ is not oriented directly along the C−Cl axis, the dipole component with this favorable orientation is sufficient to bring Cu^+ into close proximity with the Cl atom. Herein we find the discriminating feature between the behavior of $CClF_3$ and the other halocarbons. In the case of this neutral, the dipole is oriented with the negative end *away* from the Cl. We thus postulate that the significantly lower rate of depletion of $Cu^+(^3D)$ by this neutral as opposed to the other three must be the

result of an activation barrier associated with reorienting the $CClF_3$ so that Cu^+ can abstract Cl.

It also seems plausible that production of $CuCH_3^+$ is inhibited kinetically via the triplet surface for CH_3Cl, because formation of this species via a direct mechanism would require Cu^+ to approach the neutral from the positive end of the dipole resulting in a more repulsive surface. Similar kinetic impediments may exist in the formation of $CuCH_xF_y^+$ via a direct mechanism with the two HCFCs; however, our failure to observe fluorinated Cu^+−methyl analogues might also be the result of unfavorable thermochemistry. Because binding energies for $Cu-CH_2F^+$ and $CuCHF_2^+$ are not known, specific thermochemical requirements cannot be calculated; however, it seems likely that the $Cu^+-CH_xF_y$ binding will become weaker as y increases due to the electron-withdrawing influence of the fluorines. Such an effect may result in overall endothermicity for $CuCH_xF_y^+$ formation via the HCFCs. A kinetic explanation for the lack of formation of $CuCF_3^+$ is likewise unsatisfactory for $CClF_3$ because the favorable dipole orientation is one in which Cu^+ approaches the CF_3 group. The absence of reaction resulting in $CuCF_3^+$ cannot therefore be explained solely on the basis of long-range electrostatic forces. Rather, this suggests either that CF_3 abstraction is precluded due to unfavorable energetics, or that this ion−dipole geometry does not present Cu^+ with a molecular orbital suitable for bonding.

Summary

Reactions of $Cu^+(^1S)$ and $Cu^+(^3D)$ with CH_3Cl, CH_2ClF, $CHClF_2$, and $CClF_3$ have been carried out in a selected ion drift cell apparatus at room temperature. State-specificity for the obvserved products was determined using electronic state chromatography. These analyses reveal that association is the only process arising from $Cu^+(^1S)$, whereas $Cu^+(^3D)$ is responsible for a number of bimolecular products that include abstractions of Cl, H^-, and F^-. Thermochemical and quantum mechanical requirements for reaction allow us to conclude that $CuCl^+$ is the only bimolecular product that arises directly from $Cu^+(^3D)$. With all four neutrals, $CuCl^+$ initiates a series of energetically allowed and spin-allowed follow-on reactions that yield the remaining products observed to arise from $Cu^+(^3D)$. The absence of dihydrohalogenation products can be understood on the basis of unfavorable energetics from $Cu^+(^1S)$, and unfavorable spin changes with respect to formation via $Cu^+(^3D)$ because this would require the formation of a $Cl-Cu^+-CH_xF_y$ intermediate of low spin. This is consistent with behavior observed previously for the reaction of these two Cu^+ states with CH_3Br and indicates that coupling of the two reaction surfaces does not occur. This is further supported by the observation that Cu^+−methyl species are not observed in any of these reactions. Rather, the exclusive formation of $CuCl^+$ by $Cu^+(^3D)$ suggests a direct mechanism in which the metal interacts only with Cl. Rates of depletion of $Cu^+(^3D)$ by CH_3Cl and the HCFCs indicate that Cl abstraction with these neutrals is efficient; however, this process occurs at a significantly slower rate with $CClF_3$, indicating the presence of an activation barrier. We postulate that this barrier arises due to a dipole orientation that does not bring Cl into close proximity with Cu^+. Qualitatively, this mechanistic interpretation seems consistent with that reported for the reaction of $Fe^+(^4F)$ and $Fe^+(^6D)$ with CH_3Cl where diabatic reaction of $Fe^+(^6D)$ results in exclusive formation of $FeCl^+$ and formation of $FeCH_3^+$ via $Fe^+(^6D)$ occurs only as a result of an avoided crossing between the high-spin and low-spin reaction surfaces.[41] Such adiabatic behavior cannot occur in the reactions described here due to the ordering of the Cu^+ states. With respect to our previous work, we believe that a similar mechanism governs the behavior of Cu^+ with CH_3Br, because $CuBr^+$ is the only product observed to originate from $Cu^+(^3D)$ in that system also.[25]

Acknowledgment. Support for this research was provided by the National Science Foundation under Grant No. CHE-0078771.

References and Notes

(1) Armentrout, P. B.; Beauchamp, J. L. *Acc. Chem. Res.* **1989**, *22*, 315−321.
(2) Armentrout, P. B. *Science* **1991**, *251*, 175−179.
(3) Eller, K. E.; Schwarz, H. *Chem. Rev.* **1991**, *91*, 1121−1177.
(4) Armentrout, P. B. *Int. J. Mass Spectrom. Ion Processes* **2003**, *227*, 289−302.
(5) Armentrout, P. B. *Acc. Chem. Res.* **1995**, *28*, 430−436.
(6) Armentrout, P. B. in *Gas-Phase Inorganic Chemistry*; Russell, D. H., Ed.; Plenum: New York, 1989.
(7) Weisshaar, J. C. *Acc. Chem. Res.* **1993**, *26*, 213−219.
(8) Armentrout, P. B. *Annu. Rev. Phys. Chem.* **1990**, *41*, 313−344.
(9) Weisshaar, J. C. in *Advances in Chemical Physics*; Ng, C. Y., Baer, M., Eds.; Wiley and Sons Inc., New York, 1992; Vol. LXXXII.
(10) Schwarz, H. *Int. J. Mass Spectrom. Ion Processes* **2004**, *237*, 75−105.
(11) Schröder, D.; Shaik, S.; Schwarz, H. *Acc. Chem. Res.* **2000**, *33*, 139−145.
(12) Hoyau, S.; Ohanessian, G. *Chem. Phys. Lett.* **1997**, *280*, 266−272.
(13) Fisher, E. R.; Armentrout, P. B. *J. Phys. Chem.* **1990**, *94*, 1674−1683.
(14) Georgiadis, R.; Fisher, E. R.; Armentrout, P. B. *J. Am. Chem. Soc.* **1989**, *111*, 4251−4262.
(15) Elkind, J. L.; Armentrout, P. B. *J. Phys. Chem.* **1986**, *90*, 6576−6586.
(16) Rue, C.; Armentrout, P. B.; Kretzschmar, I.; Schröder, D.; Schwarz, H. *J. Phys. Chem. A* **2002**, *106*, 9788−9797.
(17) Rodgers, M. T.; Walker, B.; Armentrout, P. B. *Int. J. Mass Spectrom. Ion Processes* **1999**, *182/183*, 99−120.
(18) Irigoras, A.; Elizalde, O.; Silanes, I.; Fowler, J. E.; Ugalde, J. M. *J. Am. Chem. Soc.* **2000**, *122*, 114−122.
(19) Jones, R. W.; Staley, R. H. *J. Am. Chem. Soc.* **1980**, *102*, 3794−3798.
(20) Burnier, R. C.; Byrd, G. D.; Freiser, B. S. *Anal. Chem.* **1980**, *52*, 1641−1650.
(21) Cassady, C. J.; Freiser, B. S. *J. Am. Chem. Soc.* **1985**, *107*, 1566−1573.
(22) Eller, K; Karrass, S.; Schwarz, H. *Organometallics* **1992**, *11*, 1637−1646.
(23) Eller, K.; Schröder, D.; Schwarz, H. *J. Am. Chem. Soc.* **1992**, *114*, 6173−6182.
(24) Schalley, C. A.; Schröder, D.; Schwarz, H. *Organometallics* **1995**, *14*, 317−326.
(25) Taylor, W. S.; May, J. C.; Lasater, A. S. *J. Phys. Chem. A* **2003**, *107*, 2209−2215.
(26) Kemper, P. R.; Bowers, M. T. *J. Phys. Chem.* **1991**, *95*, 5134−5146.
(27) Taylor, W. S.; Campbell, A. S.; Barnas, D. F.; Babcock, L. M.; Linder, C. B. *J. Phys. Chem. A* **1997**, *101*, 2654−2661.
(28) Taylor, W. S.; Everett, W. R.; Babcock, L. M.; McNeal, T. L. *Int. J. Mass Spectrom. Ion Processes* **1993**, *125*, 45−54.
(29) Taylor, W. S.; Spicer, E. M.; Barnas, D. F. *J. Phys. Chem. A* **1999**, *103*, 643−650.
(30) Lias, S. G. .Ionization Energy Evaluation. In *NIST Chemistry WebBook*; NIST Standard Reference Database Number 69; Linstrom, P. J., Mallard, W. G., Eds.; National Institute of Standards and Technology: Gaithersburg MD, 20899, March 2003 (http://webbook.nist.gov).
(31) Lias, S. G.; Levin, R. D.; Kafafi, S. A. .Ion Energetics Data. In *NIST Chemistry WebBook*; NIST Standard Reference Database Number 69; Linstrom, P. J., Mallard, W. G., Eds.; National Institute of Standards and Technology: Gaithersburg MD, 20899, March 2003 (http://webbook.nist.gov).
(32) Lias, S. G.; Bartmess, J. E.; Liebman, J. F.; Holmes, J. L.; Levin, R. D.; Mallard, W. G. Ion Energetics Data. In *NIST Chemistry WebBook*; NIST Standard Reference Database Number 69; Linstrom, P. J., Mallard, W. G., Eds.; National Institute of Standards and Technology: Gaithersburg MD, 20899, March 2003 (http://webbook.nist.gov).
(33) Lias, S. G.; Liebman, J. F. Ion Energetics Data. In *NIST Chemistry WebBook*; NIST Standard Reference Database Number 69; Linstrom, P.

J., Mallard, W. G., Eds.; National Institute of Standards and Technology: Gaithersburg MD, 20899, March 2003 (http://webbook.nist.gov).

(34) Rosenstock, H. M.; Draxl, K.; Steiner, B. W.; Herron, J. T. Ion Energetics Data. In *NIST Chemistry WebBook*; NIST Standard Reference Database Number 69; Linstrom, P. J., Mallard, W. G., Eds.; National Institute of Standards and Technology: Gaithersburg MD, 20899, March 2003 (http://webbook.nist.gov).

(35) van Koppen, P. A. M.; Kemper, P. R.; Bowers, M. T. In *Organometallic Ion Chemistry*; Freiser, B. S., Ed.; Kluwer Academic Publishers: Boston, 1996.

(36) Feber, R. C. Los Alamos Report LA-3164, 1965.

(37) Griffiths, W. J.; Harris, F. M.; Barton, J. D. *Rapid Commun. Mass Spectrom.* **1989**, *3*, 283−285.

(38) Langford, M. L.; Harris, F. M. *Int. J. Mass Spectrom. Ion Phys.* **1990**, *96*, 111−113.

(39) Su. T; Bowers, M. T. *Int. J. Mass Spectrom. Ion Phys.* **1973**, *12*, 347−356.

(40) Fisher, E. R.; Sunderlin, L. S.; Armentrout, P. B. *J. Phys. Chem.* **1989**, *93*, 7375−7382.

(41) Fisher, E. R.; Sunderlin, L. S.; Armentrout, P. B. *J. Phys. Chem.* **1989**, *93*, 7382−7387.